Lamellar/Inverted Cubic (L_α/Q_{II}) Phase Transition in N-Methylated Dioleoylphosphatidylethanolamine

D. P. Siegel* and J. L. Banschbach

Miami Valley Laboratories, Procter & Gamble Company, P.O. Box 398707, Cincinnati, Ohio 45239-8707

Received January 18, 1990; Revised Manuscript Received April 2, 1990

ABSTRACT: Inverted cubic (Q_{II}) phases form in hydrated N-methylated dioleoylphosphatidylethanolamine (DOPE-Me). Previous work indicated that Q_{II} phases in this and other systems might be metastable structures. Whether or not Q_{II} phases are stable has important implications for models of the factors determining the relative stability of bilayer and nonbilayer phases and of the mechanisms of transitions between those phases. Here, using X-ray diffraction and very slow scan rate differential scanning calorimetry (DSC), we show that thermodynamically stable Q_{II} phases form slowly during incubation of multilamellar samples of DOPE-Me at constant temperature. The equilibrium L_α/Q_{II} phase transition temperature is 62.2 ± 1 °C. The transition enthalpy is 174 ± 34 cal/mol, about two-thirds of the L_α/H_{II} transition enthalpy observed at faster scan rates. This implies that the curvature free energy of lipids in Q_{II} phases is substantially lower than in L_α phases and that this reduction is substantial compared to the reduction achieved in the H_{II} phase. The L_α/Q_{II} transition is slow and is not reliably detected with DSC until the temperature scan rate is reduced to ca. 1 °C/h. At faster scan rates, the H_{II} phase forms at a reproducible temperature of 66 °C. This H_{II} phase is metastable until ca. 72–79 °C, where the equilibrium Q_{II}/H_{II} transition seems to occur. These results, as well as the induction of Q_{II} phases in similar systems by temperature cycling (observed by others), are consistent with a theory of $L_\alpha/Q_{II}/H_{II}$ transition mechanisms proposed earlier (Siegel, 1986c).

Inverted cubic (Q_{II})[1] phases have been observed in many phospholipid systems [for an excellent review, see Lindblom and Rilfors (1989)]. Q_{II} phases and the mechanism of lamellar (L_α)/Q_{II} phase transitions are of interest for several reasons. First, study of these phases increases our knowledge of the factors determining inverted phase stability in general [e.g., see Gruner et al. (1988) and Anderson et al. (1988)] and of the mechanisms of bilayer/nonbilayer phase transitions (Siegel, 1986a–c). Second, dynamic processes in phospholipid membranes can be strongly affected by proximity of the system to L_α/Q_{II} phase boundaries. For example, intermediates in L_α/Q_{II} transitions also mediate membrane fusion (Ellens et al., 1989; Siegel et al., 1989a). It is possible that the susceptibility of biomembranes to fusion is controlled by small changes in membrane composition that permit formation of Q_{II} phase precursors (e.g., by diglyceride production; Siegel et al., 1989b). It has also been suggested that, near L_α/Q_{II} phase boundaries, the spontaneous radii of curvature of lipid interfaces are optimal for the function of some membrane-bound or membrane-modifying enzymes [e.g., Hui and Sen (1989)]. The lipid compositions of at least some biomembranes are regulated in vivo so as to maintain the composition near the L_α/Q_{II} phase boundary at the growth temperature, and some biomembrane structures resemble cubic-phase lattices [references in Lindblom and Rilfors (1989)].

Transitions between L_α and Q_{II} phases are often profoundly hysteretic. Gruner et al. (1988) found that Q_{II} phases in N-methylated dioleoylphosphatidylethanolamine (DOPE-Me)[2] formed only after months of incubation at temperatures below T_H, the temperature at which an L_α/H_{II} phase transition is observed. In many systems, the morphology and ^{31}P NMR resonances associated with Q_{II} phases or their precursors (so-called isotropic phases) can persist after the systems are cooled far below the temperatures at which these phenomena first appear [e.g., Gagné et al. (1985), Gruner et al. (1988), and Ellens et al. (1989)]. Moreover, Shyamsunder et al. (1988) showed that, in a system that does not form Q_{II} phases during long incubations at constant temperature, exhaustive temperature cycling through T_H can form a Q_{II} phase. Findings like these suggest that Q_{II} phases in phospholipids could be metastable structures, instead of thermodynamically stable phases (Siegel, 1986c). Shyamsunder et al. (1988) also noted that their data did not exclude this possibility.

In the present work, we use differential scanning calorimetry and X-ray diffraction to show that a Q_{II} phase is thermodynamically stable in DOPE-Me within a temperature interval starting at 62.2 ± 1 °C. The Q_{II} phases that form are Q_{II}^{224} and Q_{II}^{230}, depending on the water content of the samples. These phases were detected via X-ray diffraction after incubations for several hours at temperatures of 61–62 °C. We will discuss these findings and the findings of Shyamsunder

[1] We use the same system of inverted cubic phase nomenclature as Gulik et al. (1985). These phases are denoted by the symbol Q_{II}^n, where n is the space group number of the structure in *International Tables for X-ray Crystallography* (1968). We have added the subscript to indicate that these phases are inverted (i.e., water labyrinths enclosed within bilayer structures, as opposed to arrays of lipid micelles packed within a water continuum), as has been established by morphological and NMR techniques [e.g., see Lindblom and Rilfors (1989)]. Q_{II}^{224} corresponds to an inverted cubic phase of space group *Pn3m*, Q_{II}^{230} to a phase of space group *Ia3d*, and Q_{II}^{229} to a phase of space group *Im3m*. The symbol Q_{II} is used to indicate either these structures in general or another inverted cubic phase based on an infinite periodic minimal surface geometry of different symmetry.

[2] Abbreviations: DOPE, dioleoylphosphatidylethanolamine; DOPE-Me, N-methylated dioleoylphosphatidylethanolamine; DSC, differential scanning calorimetry; EDTA, ethylenediaminetetraacetate; ILA, interlamellar attachment; LPC, 1-oleoyllysophosphatidylcholine; LPE, 1-oleoyllysophosphatidylethanolamine; OA, oleic acid; NMR, nuclear magnetic resonance spectroscopy; T_H, L_α/H_{II} phase transition temperature (at fast temperature scan rates); T_Q, L_α/Q_{II} phase transition temperature; T_{QH}, Q_{II}/H_{II} phase transition temperature; TES, 2-[[tris(hydroxymethyl)methyl]amino]ethanesulfonic acid; TLC, thin-layer chromatography.

0006-2960/90/0429-5975$02.50/0

et al. (1988) in the light of a proposed L_α/Q_{II} phase transition mechanism (Siegel, 1986c) and recent theoretical work on the relative stability of Q_{II}, H_{II}, and L_α phases (Anderson et al., 1988).

Materials and Methods

Materials. N-Methylated dioleoylphosphatidylethanolamine (DOPE-Me), N,N-dimethylated dioleoylphosphatidylethanolamine, 1-oleoyllysophosphatidylethanolamine (LPE), and 1-oleoyllysophosphatidylcholine (LPC) were all purchased from Avanti Polar Lipids, Inc. (Pelham, AL) and were used without further purification. At our request, the manufacturer treated the DOPE-Me supplied to us with a further chromatography step (an additional silica gel column in 2:1 chloroform/methanol, followed by a Fulch partition) to remove trace impurities. Oleic acid (OA) was purchased from Sigma Chemical Co. (St. Louis, MO). All salts used in the buffer solutions were reagent grade. Cyclohexane (spectrophotometric grade) was obtained from Aldrich Chemical Co., and reagent-grade chloroform was obtained from Fisher Scientific.

The DOPE-Me was usually about 99.7% pure as judged by TLC (see below). The T_H of DOPE-Me is sensitive to low levels of some impurities (Siegel et al., 1989b,c; Ellens et al., 1989). Therefore, as a rough check of the purity of each lot of DOPE-Me, T_H was measured in dilute samples in TES buffer (below) by use of the liquid-sample cell of a MC-2 differential scanning calorimeter (Microcal, Inc., Northampton, MA) scanning at 13 °C/h. The value of T_H as determined from seven lots is 66.1 ± 0.5 °C (Ellens et al., 1989; Siegel et al., 1989b,c). No lot was used in this study if the measured T_H fell outside this range or if total impurities in excess of ca. 0.5% were detected via TLC. Using samples spiked with known amounts of fatty acids or lysolipids, we found that the TLC procedures could detect less than 0.2 wt % of those contaminants. Most lots of DOPE-Me fulfilled these requirements.

Buffers. Lipids were dispersed in (i) 100 mM NaCl, 20 mM TES (pH 7.4), and 0.1 mM EDTA or (ii) 100 mM NaCl, 50 mM acetate (pH 4.5), and 0.1 mM EDTA, as indicated. Buffers were made with water from a Milli-Q purification system (Millipore Corp., Bedford, MA).

Differential Scanning Calorimetry. For single-component DOPE-Me samples, a known weight of lyophilized DOPE-Me was hydrated in an appropriate weight of TES buffer in the MC-2 solid-sample cells in order to yield final lipid concentrations of 33, 40, 50, or 60 wt %. Samples contained as much as 166 mg of DOPE-Me for experiments at slow temperature scan rates. The sample cells were sealed and equilibrated for 2–3 h at 4 °C. They were then agitated by extensive vortex mixing and subjected to seven freeze/thaw cycles (dry ice and a 40 °C water bath). Thermograms were obtained in the solid-sample head of the MC-2, while scanning at rates between 1 and 9 °C/h. Scan rates slower than 9 °C/h were obtained by modifying the instrument according to instructions from the manufacturer.

When using the solid-sample head of the MC-2 calorimeter, we found that a flatter base line could sometimes be obtained by closely matching the heat capacities of the reference and sample cells with the following procedure. We used an amount of N-dimethylated dioleoylphosphatidylethanolamine equal to the weight of the DOPE-Me in the sample cell, hydrated with the same amount of buffer, in the reference cell. The temperature-dependent heat capacities of these two very similar lipids should be similar. Separate experiments verified the absence of endotherms due to the dimethylated lipid in this temperature range (data not shown). Gruner et al. (1988) also verified that no phase transitions occur in the dimethylated lipid between 50 and 80 °C.

For multicomponent samples, known weights of DOPE-Me and lipid additives were cosolubilized in chloroform, and the solvent was removed under high vacuum. The lipid film was hydrated in excess buffer by vortex mixing and several freeze/thaw cycles. The resulting suspension was loaded into the liquid-sample cell of the MC-2 and scanned at 13 °C/h.

X-ray Diffraction Samples. Samples were prepared in glass capillaries (0.9-mm o.d.; Charles Supper, Inc., Natick, MA). The lipid was dissolved in cyclohexane and then transferred to the capillaries, and the solvent was removed under high vacuum for ca. 3 h. The samples were hydrated with a known volume of TES buffer and flame sealed. The capillaries were placed in small centrifuge tubes filled with water, which were then centrifuged at 1500*g* for 1.5 min. The capillaries were inverted in the water-filled tubes and centrifuged again. The capillaries were centrifuged a total of 10 times. This mechanically mixed the samples to apparent homogeneity. The tubes were then inserted into water baths at the desired incubation temperature. The temperatures in the incubation bath were spatially uniform and at the desired value to within an accuracy of 0.2 °C.

Capillaries were loaded into a thermostated sample holder at the expeimental temperature (±0.2 °C), and diffraction patterns were obtained on a Rigaku RH100 rotating-anode X-ray generator with a flat-film camera. The sample-to-film distance was 30 cm, and films were typically exposed for 3 h.

Analysis of Samples for Hydrolysis Products. DOPE-Me samples were incubated in glass capillaries at 61 °C under the same conditions used for X-ray specimens. Capillaries were broken open, the contents were dissolved in appropriate solvents, and the lipid composition was analyzed by thin-layer chromatography (TLC). Both one- and two-dimensional TLC experiments were performed using silica gel G plates (Analtech, Newark, NJ). Both the solvent systems used were pyridine/toluene/water = 95/85/15 (by volume) and chloroform/methanol/water/formic acid = 130/60/8/1 (by volume). Spots were visualized by spraying the plates with 25% sulfuric acid and heating to 260 °C for 15 min. Experiments in which known amounts of oleic acid or lysophospholipid were added to the DOPE-Me showed that less than 0.2 wt % of these compounds was detectable.

Results

Differential Scanning Calorimetry. In the course of earlier DSC studies of DOPE-Me, Ellens et al. (1989) and Siegel et al. (1989b) observed poorly reproducible shoulders on the low-temperature sides of L_α/H_{II} transition endotherms. These features occurred near 60 °C when the temperature scan rate was 13 °C/h or slower. An example is shown in Figure 1A. It was suggested that these small features might indicate partial transitions to the Q_{II} phase or Q_{II} phase precursors. Theory indicates that L_α/Q_{II} transitions can be very slow and hysteretic and that these transitions should proceed more readily in samples with higher lipid concentrations (Siegel, 1986c). Therefore, we investigated this system more closely, using concentrated samples in the solid-sample head of our Microcal MC-2 calorimeter and slower temperature scan rates.

At 9 °C/h, some of these higher concentration samples (33 wt % DOPE-Me in TES buffer) yield small, well-defined endotherms at 61.2–61.6 °C (Figure 1B), as well as the familiar endotherm corresponding to H_{II} phase evolution at 66 °C (Ellens et al., 1989). The combined enthalpy of the two endotherms is ca. 300 cal/mol. That is roughly the enthalpy

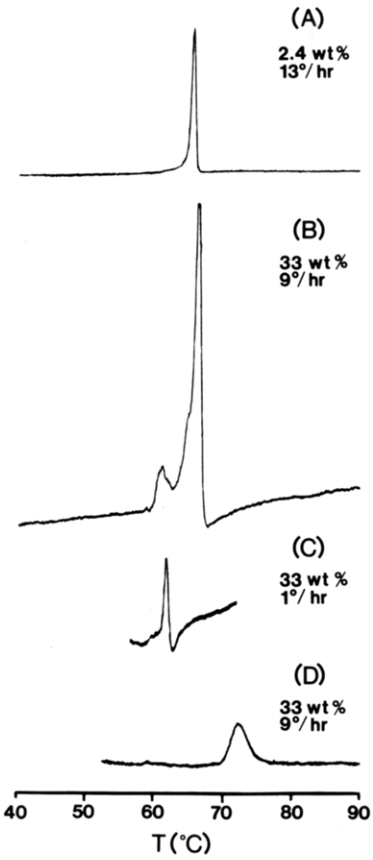

FIGURE 1: DSC thermograms of DOPE-Me samples. The sensitivities and sample size are different in each trace, so that each is on a different vertical scale. (A) Dilute dispersion scanned at 13 °C/h. The endotherm at 66 °C corresponds to the L_α/H_{II} phase transition. The transition enthalpy is 265 cal/mol in this case. Note the low-temperature shoulder. (B) 33 wt % DOPE-Me scanned at 8.8 °C/h. The combined enthalpy of the two endotherms is ca. 300 cal/mol. (C) 33 wt % DOPE-Me scanned at 1.1 °C/h. Only one endotherm (at 61.7 °C) is observed below 72 °C, with an enthalpy of 160 cal/mol. The sample was preincubated at 56 °C for 1 h before the DSC experiment. (D) 33 wt % DOPE-Me preincubated at 61.1 °C for 18 h and then scanned from 50 °C at 8.7 °C/h. A single, broad endotherm is observed at 72 °C with an enthalpy of 160 cal/mol.

of samples with single peaks at T_H, or in dilute suspensions of DOPE-Me (255 ± 23 cal/mol, 13 trials). The enthalpy of the lower temperature endotherm represents only about 15% of the total.

The low-temperature endotherm was more pronounced at slower temperature scan rates and grew at the expense of the endotherm at 66 °C. Low-temperature endotherms were always observed when 33 wt % samples were preincubated at temperatures close to 55 °C for 1 h before the DSC experiment. Figure 1C is a thermogram obtained at 1.1 °C/h. A single endotherm occurs at 61.7 °C. The dip below base line on the high-temperature side of the endotherm is instrumental in origin and reflects the high heat capacity of the sample (166 mg of DOPE-Me). Note that no other endotherms appear below 72 °C. In five samples examined at this temperature scan rate, the onset and peak temperatures of the endotherm were 61.3 ± 0.9 and 62.2 ± 1.0 °C, respectively. The enthalpy was 174 ± 34 cal/mol.

Finally, we wished to determine whether or not the phase that forms at 61–62 °C in 33 wt % samples undergoes a phase transition at higher temperatures. We incubated 33 wt % samples of DOPE-Me at 61 °C for 18–20 h. We then obtained thermograms of these samples, scanning at 9 °C/h between 50 and 90 °C. In both samples treated in this manner, only a single endotherm at 72 °C was observed (Figure 1D),

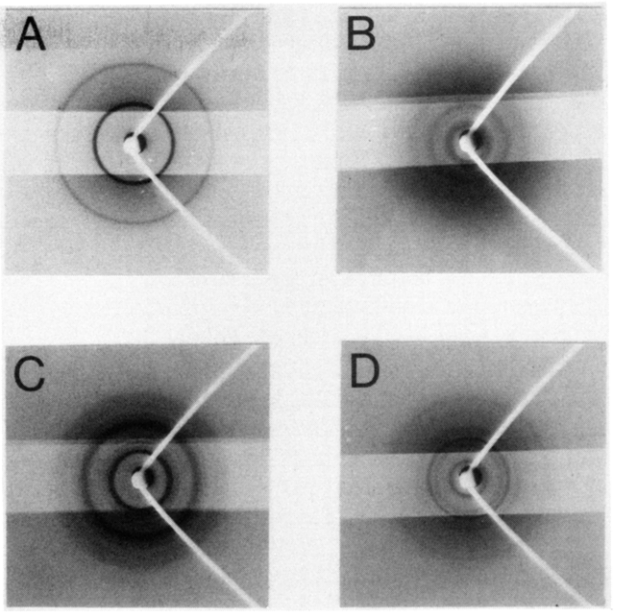

FIGURE 2: X-ray diffraction patterns obtained from samples of DOPE-Me. (A) 33 wt % DOPE-Me after incubation at 59.6 °C for 18 h. The powder pattern is that of an L_α phase with an interlamellar spacing of 62.5 Å. (B) 33 wt % DOPE-Me after incubation at 61 °C for 24 h. The powder pattern is consistent with a Q_{II}^{224} (*Pn3m*) phase (lattice constant = 192 Å). (C) 50 wt % DOPE-Me after 18 h at 61.0 °C. The pattern is consistent with the coexistence of a Q_{II}^{230} (*Ia3d*) phase (lattice constant = 204 Å) and an H_{II} phase. (D) 40 wt % DOPE-Me after 45 h at 58 °C. The powder pattern is consistent with the coexistence of an L_α phase (spacing of 62 Å; third- and fifth-smallest rings) with a weakly diffracting lattice of unknown symmetry and large lattice constant. The smallest angle reflection in this pattern corresponds to an interplane distance of approximately 145 Å.

with an apparent transition enthalpy of about 150 cal/mol. In two other cases, samples were incubated and scanned at 1 °C/h like the sample in Figure 1C, but the scan was permitted to continue to higher temperatures. Both of these thermograms contained a broad, poorly defined endotherm in addition to the one at around 62 °C, centered at 74 or 79 °C (data not shown).

The results of these calorimetric studies indicate that there is a hysteretic transition with an excess enthalpy occurring in DOPE-Me within a narrow temperature interval at 62.2 ± 1 °C. The transition is not reliably detected until the temperature scan rate is reduced to ca. 1 °C/h. This suggests that the transition proceeds on the time scale of the temperature scan across the width of the endotherm in Figure 1C (ca. 1 h). The phase that is formed under these circumstances appears to be stable up to ca. 72–79 °C.

X-ray Diffraction. Samples containing 20–50 wt % DOPE-Me were incubated at 58.0, 59.6, 61.0, 61.7, and 65.0 °C (all ±0.2 °C). X-ray diffraction patterns of samples incubated at 58.0 and 59.6 °C for 20 h or less were powder patterns consistent with diffraction from an L_α phase lattice (Figure 2A). The interbilayer spacing was 62.6 ± 1.0 Å, consistent with the value reported by Gruner et al. (1988).

Samples incubated at 61.0 and 61.7 °C yielded very different powder patterns. Samples containing 20 and 33 wt % DOPE-Me yielded powder patterns of four to five rings consistent with diffraction from a cubic *Pn3m* lattice (Q_{II}^{224} phase). These powder patterns were obtained from samples incubated for 5 h or longer (including the duration of the X-ray exposure). We did not investigate samples incubated for shorter periods. The spacings were in the ratio $1/\sqrt{2}:1/\sqrt{3}:1/\sqrt{6}:1/\sqrt{9}:1/\sqrt{10}$. This series of lines is missing the

200 ($1/\sqrt{4}$) and 220 ($1/\sqrt{8}$) reflections of the series corresponding to a lattice of *Pn3m* symmetry (*International Tables for X-ray Crystallography*, 1968; Lindblom & Rilfors, 1989). A weak line corresponding to the 200 reflection was observed in some cases. Gruner et al. (1988) and Shyamsunder et al. (1988), in studies of Q_{II}^{224} phases in DOPE-Me and DOPE performed with more sensitive detectors, showed that the intensities of the 200 and 220 reflections are small compared to the intensities of the others. Those lines are probably missing from our patterns for that reason. While we cannot unambiguously establish the symmetry group of the Q_{II} phase from our data, it is most probably *Pn3m* (Q_{II}^{224}).

The unit-cell constant of the Q_{II}^{224} phase that formed at 61–62 °C in 33 wt % DOPE-Me samples was somewhat variable. Values usually fell between 188 and 198 Å, although values as large as 212 Å were infrequently observed. Similar variability has been noted in Q_{II}^{224} phases formed by temperature cycling DOPE (Shyamsunder et al., 1988) and DOPE-Me (Gruner et al., 1988). The Q_{II}^{224} phase persisted for as long as 27 h at 61–62 °C. A similar lattice was observed in samples incubated for 21–24 h at 65 °C.

Samples with higher lipid contents yielded more complex powder patterns. Samples that were 50 or 60 wt % DOPE-Me, incubated at 61 °C for 18–23 h, yielded powder patterns consistent with the coexistence of a Q_{II} phase of *Ia3d* symmetry (Q_{II}^{230}) with traces of H_{II} phase. An example is shown in Figure 2C. This pattern contains seven of the first eight reflections expected for an *Ia3d* lattice ($1/\sqrt{3}$:$1/\sqrt{4}$:$1/\sqrt{7}$:$1/\sqrt{8}$:$1/\sqrt{10}$:$1/\sqrt{11}$:$1/\sqrt{13}$), missing the $1/\sqrt{12}$ reflection (*International Tables for X-ray Crystallography*, 1968; Lindblom & Rilfors, 1989). The unit-cell constant for this lattice is 204 Å. The pattern also contains three reflections (in the ratio 1:$1/\sqrt{3}$:$1/\sqrt{4}$) consistent with an H_{II} phase lattice. The H_{II} tube diameter is 73 Å, close to the value of 74 Å observed at about 65 °C by Gruner et al. (1988). Since 61 °C is below T_H and the water content of the samples is larger than that of the H_{II} phase [ca. 20%, on the basis of data in Gruner et al. (1988)], this H_{II} phase is not at equilibrium. H_{II} phase probably formed due to nonuniform hydration or incomplete mixing of these concentrated samples. DSC studies of 60 wt % samples also indicated nonuniform sample hydration. In 60 wt % samples, L_α/Q_{II} endotherms occurred at 60 ± 2 °C, but L_α/H_{II} endotherms also appeared at 64 ± 1 °C (data not shown), which is below T_H as observed in more hydrated samples. On account of these difficulties, 50 or 60 wt % samples were not studied in detail.

We investigated the high-temperature behavior of one sample of the Q_{II}^{224} phase in 33 wt % DOPE-Me. A sample was incubated for 16 h at 62 °C. An X-ray diffraction pattern after this incubation period consisted only of the first four reflections of a Q_{II}^{224} powder pattern. The capillary was then heated to 71.4 °C, and another X-ray diffraction pattern was obtained after 0.5 h of equilibration time. This pattern consisted of a faint series of lines compatible with a Q_{II}^{224} phase and an intense series of lines consistent with an H_{II} phase (data not shown). The same capillary was subsequently heated to 80.7 °C and another diffraction pattern obtained, which was qualitatively similar (data not shown). The apparent lattice constant of the Q_{II}^{224} phase decreased from ca. 190 Å at 62 °C to 155 and 130 Å at 71.4 and 80.7 °C, respectively. The lattice constant of the H_{II} phase at 71.4 and 80.7 °C was ca. 73.7 and 72.5 Å, respectively, in good agreement with values obtained by Gruner et al. (1988).

DOPE-Me samples hydrolyze to some extent under the incubation conditions employed in this study. We therefore determined the extent and effects of such hydrolysis. Samples containing 33 wt % DOPE-Me in X-ray diffraction capillaries were analyzed to determine the extent of hydrolysis after incubation at 61 °C. After 20 h, 1.5 mol % of the DOPE-Me had hydrolyzed, and 3 mol % had hydrolyzed after 40 h. We were surprised to observe that samples incubated in sealed flasks or sealed MC-2 solid-sample cells underwent almost no hydrolysis under these conditions.

These studies indicate that very little hydrolysis occurred in samples that formed detectable levels of Q_{II} phase and that low levels of hydrolysis products have small effects on T_Q. For example, samples of DOPE-Me (33 wt %) incubated at 58 or 59.6 °C did not yield Q_{II} diffraction patterns even after 20 h, whereas identical samples incubated at 61.0 or 61.7 °C formed Q_{II}^{224} lattices within less than 5 h. We would expect less than 0.4 mol % of the DOPE-Me to have hydrolyzed under the latter circumstances. Moreover, the L_α/Q_{II}^{224} endotherm in Figure 1B was obtained after only ca. 2 h near T_Q. Since samples incubated in sealed DSC cells underwent much less hydrolysis than samples incubated in capillaries, we estimate that 0.1 mol % or less of the DOPE-Me hydrolyzed in that case. We infer that accumulation of DOPE-Me hydrolysis products is not required for Q_{II} phase formation.

Hydrolysis products significantly perturbed the behavior of samples incubated for more than 20 h. We determined the effects of hydrolysis products (modeled as a mixture of OA, LPE, and LPC in the molar ratio 3/2/1) on T_H of dilute samples of DOPE-Me in pH 4.5 buffer using DSC. The experiments were run in pH 4.5 buffer since 33 wt % DOPE-Me samples are poorly pH buffered and, after ca. 1% hydrolysis has occurred, most of the OA will be protonated. Hydrolysis products reduced T_H by ca. 1 °C per mole percent at pH 4.5 (data not shown). Thus, the accumulation of hydrolysis products during long incubations near 60 °C increased the tendency toward inverted phase formation. For example, DOPE-Me (33 wt %) samples incubated at 58 °C for 44–68 h yielded powder diffraction patterns consisting of reflections at spacings of ca. 130–150, 70–80, and 45–55 Å, as well as L_α phase reflections (Figure 2D). These reflections probably arise from a poorly ordered Q_{II} phase, mixtures of different Q_{II} phases, or Q_{II} phase precursors.

The accumulation of hydrolysis products may also change the relative stability of different Q_{II} phase lattices. While 33 wt % samples incubated for only a few hours at 61 °C yielded well-defined Q_{II}^{224} phase patterns, a sample incubated for 45 h yielded a disordered pattern like that in Figure 2D. Another sample incubated for 51 h at 61 °C yielded a Q_{II}^{230} phase pattern (lattice constant = 250 Å; data not shown). This suggests a progressive change from *Pn3m* to *Ia3d* symmetry for the Q_{II} phase with increasing concentrations of DOPE-Me hydrolysis products.

Discussion

The results reported here indicate that a Q_{II}^{224} phase forms in DOPE-Me samples incubated for several hours at a temperture of 61–62 °C. The X-ray diffraction data indicate that the width of the transition is about 1.4 °C (panel A vs panel B of Figure 2), and the endotherms observed with DSC generally have widths at half-height of 0.7 °C (e.g., Figure 1C). The excess enthalpy and narrow transition temperature interval indicate that the L_α to Q_{II}^{224} transition at 62.2 ± 1 °C is a low-order phase transition and that the Q_{II}^{224} phase is thermodynamically stable with respect to the L_α phase starting at that temperature.

DSC data (e.g., Figure 1D) show that the Q_{II}^{224} phase undergoes a broad transition at around 72–79 °C. X-ray data

indicate that the Q_{II}^{224} phase coexists with H_{II} phase at both 71.4 and 80.7 °C. We infer that a Q_{II}^{224}/H_{II} phase transition occurs at ca. 72–79 °C. The putative Q_{II}^{244}/H_{II} transition temperature at 72–79 °C is also consistent with the measured enthalpies of the L_α/H_{II} and L_α/Q_{II}^{224} transitions (255 ± 23 and 174 ± 34 cal/mol, respectively). The chemical potential differences between the L_α and Q_{II}^{224} phases and between the L_α and H_{II} phases can be expressed in terms of the transition enthalpies for temperatures near T_H and T_Q. Equating these two expressions, one can estimate T_{QH}, the temperature of the equilibrium Q_{II}^{224}/H_{II} phase transition:

$$T_{QH} \approx \frac{Q - 1}{Q/T_H - 1/T_Q}$$

where Q is the ratio of the enthalpy at T_H in rapidly heated dilute systems (where no Q_{II}^{224} phase forms) to the enthalpy at T_Q. This equation predicts a T_{QH} of 75 °C. (The range is 72–82 °C for a 15% uncertainty in Q at the mean value of T_Q and 73–78 °C for a 1 °C error in T_Q at the mean value of Q.) This value is in agreement with the DSC and X-ray diffraction data.

The persistence of the Q_{II}^{224} diffraction pattern over a broad temperature interval (71.4–80.7 °C) is probably due to the width or hysteresis of the Q_{II}/H_{II} transition. Q_{II} phases and structures believed to be their precursors persist at temperatures far above T_H, at least under some conditions (Gruner et al., 1988; Shyamsunder et al., 1988; Ellens et al., 1988).

An interesting implication of the apparent Q_{II}/H_{II} transition at 72–79 °C (T_{QH}) is that the H_{II} phase that forms after brief incubations in dilute DOPE-Me suspensions (T_H = 66.1 ± 0.5 °C) is actually metastable between T_H and T_{QH}. This represents a cautionary tale concerning the reproducibility of nonequilibrium behavior. The L_α/Q_{II}^{224} transition requires hours to occur and cannot occur in rapidly heated samples. In contrast, the L_α/H_{II} transition occurs in seconds in DOPE-Me (Siegel et al., 1989b). Presumably, the H_{II}/Q_{II} transition is sufficiently slow and hysteretic to prevent rapid evolution of Q_{II} phase between T_Q and T_H under these circumstances.

Gruner et al. (1988) also observed Q_{II} phases in DOPE-Me. These workers observed progressive disordering of the L_α phase lattice over the course of 20 h at 55 °C. They observed diffraction from a well-ordered Q_{II}^{224} phase in a 33 wt % sample that had been at room temperature for 1.5 years. Gruner et al. reported that approximately 2 mol % of the DOPE-Me sample had hydrolyzed during that time. These results are qualitatively compatible with ours. Since T_Q appears to be 61–62 °C, Gruner et al. did not observe Q_{II} lattices within hours at 55 °C. However, the slow hydrolysis of the samples apparently encouraged the formation of nonbilayer phases, consistent with our own findings. This accounts for the gradual disordering of the L_α phase lattice at 55 °C that they observed, similar to the behavior we observed in samples incubated longer than 20 h at 58 °C (Figure 2D). Sample hydrolysis also probably explains the formation of the Q_{II} phase that Gruner et al. observed in a sample incubated for 1.5 years.

Previously, it was suggested that Q_{II} phases in phospholipid systems might be metastable structures (Siegel, 1986c). Moreover, in DOPE, Q_{II} phase forms in a manner that suggests metastability. In DOPE samples, Q_{II} phases do not form after as long as 2 weeks at constant temperature near T_H (M. Tate and E. Shyamsunder, personal communication). This implies that Q_{II} phases are thermodynamically unstable in DOPE. However, Shyamsunder et al. (1988) reported that Q_{II} phases could be formed in DOPE by cycling the temperature of a sample across an interval centered on T_H several hundred or thousand times. Shyamsunder et al. noted that their experiments did not exclude the possibility that Q_{II} phases formed by temperature cycling are thermodynamically metastable. The results of the present work show that thermodynamically stable Q_{II} phases arise spontaneously in DOPE-Me without temperature cycling. Why is temperature cycling required to form Q_{II} phase in DOPE and not in DOPE-Me? If the Q_{II} phase is thermodynamically unstable in DOPE, what accounts for the difference in stability in these two systems? What might these differences tell us about inverted phases and the mechanisms of lamellar/inverted phase transitions in general?

We suggest that these differences can be rationalized by a model of the transition kinetics (Siegel, 1986c) and the theory of Q_{II} phase stability developed by Anderson et al. (1988). Anderson's et al. model rationalizes the thermodynamic stability of Q_{II} phases. The kinetic model appears to explain the kinetics and what is known of the mechanism of the L_α/Q_{II} phase transition, as well as why Q_{II} phases form facilely in some systems but only after exhaustive temperature cycling in others.

The proposed L_α/Q_{II} transition mechanism is depicted in Figure 3. Catenoid intermediates called ILAs (interlamellar attachments) form between apposed L_α phase bilayers (Figure 3A). The rate of formation of ILAs is supposed to be determined by a quantity related to the spontaneous radius of curvature of the lipid monolayers (Siegel, 1986a,b). This curvature is a property of the lipid composition (Gruner et al., 1988). ILAs should form frequently in systems with curvature like DOPE-Me and rarely in systems like DOPE. ILAs were proposed to have no thermodynamic stability with respect to the L_α phase but to revert to the L_α phase only at extremely slow rates (Siegel, 1986b,c).

ILAs accumulate below T_H (Figure 3B). Maximizing the number of ILAs per unit area, subject to the constraint that ILAs are equally likely to form on each side of a given bilayer, results in formation of a primitive tetragonal array of ILAs (Figure 3C). The connectivity of the array of ILAs is equivalent to that of an inverted cubic lattice of the symmetry group $Im3m$ (Q_{II}^{229}), shown in Figure 3D. In this approximate model, the curvature free energy of the structures in panels C and D of Figure 3 are very nearly equal, and the Q_{II}^{229} phase would form due to fluctuations in the curvature of the bilayer. Note that the thermodynamic stability of Q_{II} phases cannot drive ILA formation, since these phases form on a time scale of hours (present work; Gruner et al., 1988), whereas ILAs are detected within seconds (Siegel et al., 1989a).

There are two driving forces for formation of both the ILA array and the Q_{II}^{229} phase. The first is simply thermodynamic stability of the final Q_{II} phase. The second is imposed by the water content of the sample. Isolated ILAs increase the local spacing between apposed bilayers severalfold (Siegel, 1986b,c), increasing the local water concentration by a similar factor. The water content of the ILA array is slightly smaller, and the water content of Q_{II}^{229} ($Im3m$) is in turn smaller than that of the ILA array. If the bulk water content of the sample is low or the rate of water transport within the L_α phase is slow, the system will tend to segregate ILAs into progressively more concentrated clusters, corresponding to the sequence of structures in panels B–D of Figure 3. Siegel (1986c) speculated that the Q_{II}^{229} phase could easily interconvert with Q_{II}^{224} and Q_{II}^{230} (Figure 3D). Interconversion of these phases involves only bending of the constituent bilayers, not creation or destruction of bilayer interconnections (Andersson et al., 1988). Within the approximation used, these Q_{II} phases have very similar free energies, and the activation energies for in-

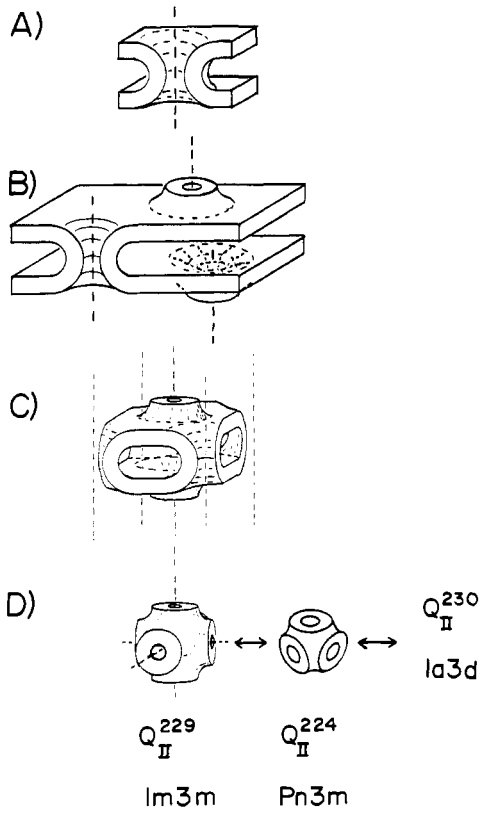

FIGURE 3: Proposed mechanism for the L_α/Q_{II} phase transition. L_α phase bilayers are drawn as single slabs. (A) Interlamellar attachments (ILAs) form between apposed L_α phase bilayers. An ILA is depicted in vertical cross section. The height of the ILAs in the direction normal to the plane of the bilayers is much larger than the equilibrium interlamellar spacing. As many ILAs form (B), the L_α phase lattice disorders. ILAs on top of and below the two apposed lamellae are shown in cross section at their narrowest point in planes parallel to the bilayers. Eventually, increase in the number of ILAs automatically leads to formation of an ILA array with a primitive tetragonal unit cell (C). This structure has the same connectivity as Q_{II}^{229} (D). Conversion into Q_{II}^{229} requires only bilayer bending. Q_{II}^{229} can probably readily interconvert with other Q_{II} phases with geometries based on bicontinuous surfaces of equivalent genus [center and right-hand side of (d)], because this process also requires only bilayer bending. The driving forces for both the primitive tetragonal array/Q_{II} transition and interconversion of different Q_{II} phases are the different thermodynamic stabilities of the Q_{II} phases (Anderson et al., 1988) and constraints imposed by the water content of the sample (Siegel, 1986c).

terconversion were assumed to be small.

This kinetic model predicts that ILAs should form readily in DOPE-Me and only rarely in DOPE during incubations near T_H, which has been verified (Siegel et al., 1989a). ILA arrays like the one in Figure 3C have also been observed in DOPE-Me, but not DOPE, via freeze–fracture electron microscopy (Ellens et al., 1989; Siegel et al., 1989a).

The model also rationalizes the induction of Q_{II} phases by temperature cycling (Shyamsunder et al., 1988). ILAs are produced in very small numbers near T_H in DOPE (Siegel et al., 1989a). However, once formed, ILAs are kinetically stable and revert to planar bilayers very slowly (Siegel, 1986b,c). This is consistent with the observed persistence of ILAs and associated isotropic ^{31}P NMR resonances when samples are cooled far below T_H [e.g., Gruner et al. (1988) and Ellens et al. (1989)]. Thus, each pass of the system through T_H accumulates more ILAs. After hundreds or thousands of cycles, enough ILAs should accumulate to form the observed DOPE Q_{II} phase as described in Figure 3. Temperature cycling also produces Q_{II} phases in DOPE-Me, but many fewer cycles are required to form Q_{II} phase (Gruner et al., 1988), probably because many more ILAs are observed to form in that system (Siegel, 1989a).

Finally, the kinetic model rationalizes the observation by Shyamsunder et al. (1988) that temperature cycling produced Q_{II} phases in DOPE samples that were 50 wt % water but not in samples containing 65% water. The Q_{II} phases produced in DOPE are probably not thermodynamically stable, since Q_{II} lattices do not form in DOPE samples incubated near T_H for 2 weeks (M. Tate and E. Shyamsunder, personal communication). For such systems, the kinetic model predicts that temperture cycling should produce Q_{II} phases only in samples with water contents substantially less than that of the ILA lattice in Figure 3C. This is because water content is then the only driving force for ordering of ILAs into lattices and Q_{II} phases (Figure 3B–D). With expressions from Siegel (1986c) and a DOPE bilayer thickness of 37 Å and a DOPE H_{II} tube diameter of 82 Å (Gruner et al., 1988), the water content of the ILA array (Figure 3C) can be estimated as ca. 66%. Therefore, the model correctly predicts that Q_{II} lattices should not be observed in samples that are 65% water. In contrast, the thermodynamic stability of the Q_{II}^{224} phase in DOPE-Me drives Q_{II} formation at both 50 and 67% water.

The insightful work of Anderson et al. (1988) rationalizes the relative thermodynamic stability of L_α, Q_{II}, and H_{II} phases. Anderson et al. used a more sophisticated model for the curvature and lipid chain-packing free energies of the lipid monolayers composing the Q_{II} phase. Q_{II} and H_{II} phases are stabilized by a reduction in the curvature free energy, whereas they are destabilized by the necessity for the lipid chains either to fill interstices in the H_{II} lattice or to accommodate variations in lipid monolayer thickness across the Q_{II} lattice.

Anderson et al. (1988) postulated that stable Q_{II}^{224} phases would form at temperatures below but close to T_H. The relative stability of Q_{II} and H_{II} phases in a given system is determined by the values of the spontaneous radius of curvature, the bending elastic constant of the lipid monolayers, a chain-packing elastic constant, and the monolayer thickness (Anderson et al., 1988). The sample water content and the Gaussian curvature elastic constant of the system may also play a role in stabilizing Q_{II} phases (Anderson et al., 1988, 1989). Presumably, the values of these parameters for DOPE either are unsuitable for Q_{II} phase formation in the relevant temperature interval or make the Q_{II} phase only very slightly more stable than L_α, so that the L_α/Q_{II} transition is extraordinarily slow.

The enthalpies of the L_α/Q_{II}^{224} and L_α/H_{II} transitions are comparable in DOPE-Me. This suggests that Q_{II}^{224} phase formation is accompanied by a substantial reduction in curvature free energy relative to the L_α phase, perhaps in the fashion suggested by Anderson et al. (1988).

Anderson et al. (1989) showed that the relative stability of different Q_{II} lattices in a given system can depend on the water content of the sample. This is consistent with the presence of Q_{II}^{224} in 33 wt % DOPE-Me samples and Q_{II}^{230} in 50 wt % samples at 61–62 °C (Figure 2B,C).

The results in this work indicate that some aspects of the kinetic model (Siegel, 1986a–c) may have to be modified. The model predicts that the first Q_{II} phase to form during the L_α/Q_{II} transition will be Q_{II}^{229} (Figure 3D). We found no evidence for Q_{II}^{229} in X-ray diffraction patterns obtained after 2–5 h of incubation at T_Q. Gruner et al. (1988) obtained some evidence for coexistence of Q_{II}^{229} with Q_{II}^{224} in DOPE-Me, but at temperatures far below T_Q and after very long incubations. It may be that Q_{II}^{229} forms only as a transient intermediate near T_Q.

It is also conceivable that ILAs assemble into Q_{II} phases via formation of ILA arrays of different symmetry than that of the array in Figure 3C. The array in Figure 3C is the first one that is encountered as the ILA density is increased. At higher ILA densities, the system would give rise to structures in which, in each original planar bilayer, the bases of ILAs pointing "up" and "down" are each arranged in long, continuous strings. Perhaps these complex geometries, or the boundaries between ILA arrays of different symmetries, contain units that can form Q_{II}^{224} or Q_{II}^{230} without prior formation of Q_{II}^{229}.

The kinetic model may also give an incomplete account of the factors determining ILA formation rates. Anderson et al. (1989) showed that when the spontaneous radius of curvature of the lipid monolayers is toward the solvent, the system can lower its curvature free energy by forming bilayer structures based on infinite periodic minimal surfaces. A minimal surface resembling ILA-like catenoid elements between lamellar sheets has recently been described (Karcher, 1988; Thomas et al., 1988). It is thus conceivable that ILAs have slight curvature stabilization with respect to the L_α phase. In that case, differences in ILA formation rates between systems could be due in part to differences in the extent of this stability, as well as to differences in the kinetic factors discussed by Siegel (1986b,c). To identify the factors controlling ILA production, we need to know more about the types and relative stabilities of minimal surface-based structures that form near L_α/H_{II} phase boundaries.

Nonlamellar structures can have important influences on the dynamics of biomembrane processes [e.g., Ellens et al. (1989), Siegel et al. (1989b), and Hui and Sen (1989)]. It is clear that we must study these structures in order to better understand the roles of lipids in biomembrane functions.

Acknowledgments

We are grateful to J. Bentz, H. Ellens, and D. Alford for helpful discussions, Ms. D. Bailey for expert TLC analysis, and to S. Williston and J. Brantz for their aid in modifying the MC-2.

References

Anderson, D. M., Gruner, S. M., & Leibler, S. (1988) *Proc. Natl. Acad. Sci. U.S.A. 85*, 5364–5368.

Anderson, D., Wennerström, H., & Olsson, U. (1989) *J. Phys. Chem. 93*, 4243–4253.

Andersson, S., Hyde, S. T., Larsson, K., & Lidin, S. (1988) *Chem. Rev. 88*, 221–242.

Ellens, H., Siegel, D. P., Alford, D., Yeagle, P. L., Boni, L., Lis, L. J., Quinn, P. J., & Bentz, J. (1989) *Biochemistry 28*, 3692–3703.

Gagné, J., Stamatatos, L., Diacovo, T., Hui, S. W., Yeagle, P. L., & Silvius, J. (1985) *Biochemistry 24*, 4400–4408.

Gruner, S. M., Tate, M. W., Kirk, G. L., So, P. T. C., Turner, D. C., Keane, D. T., Tilcock, C. P. S., & Cullis, P. R. (1988) *Biochemistry 27*, 2853–2866.

Gulik, A., Luzzati, V., De Rosa, M., & Gambacorta, A. (1985) *J. Mol. Biol. 182*, 131–149.

Hui, S. W., & Sen, A. (1989) *Proc. Natl. Acad. Sci. U.S.A. 86*, 5825–5829.

International Tables for X-ray Crystallography (1968) Kynoch Press, Birmingham, England.

Karcher, H. (1988) *Manuscr. Math. 62*, 83–114.

Lindblom, G., & Rilfors, L. (1989) *Biochim. Biophys. Acta 988*, 221–256.

Shyamsunder, E., Gruner, S. M., Tate, M. W., Turner, D. C., So, P. T. C., & Tilcock, C. P. S. (1988) *Biochemistry 27*, 2332–2336.

Siegel, D. P. (1986a) *Biophys. J. 49*, 1155–1170.

Siegel, D. P. (1986b) *Biophys. J. 49*, 1171–1183.

Siegel, D. P. (1986c) *Chem. Phys. Lipids 42*, 279–301.

Siegel, D. P., Burns, J. L., Chestnut, M. H., & Talmon, Y. (1989a) *Biophy. J. 56*, 161–169.

Siegel, D. P., Banschbach, J. L., Alford, D., Ellens, H., Lis, L. J., Quinn, P. J., Yeagle, P. L., & Bentz, J. (1989b) *Biochemistry 28*, 3703–3709.

Siegel, D. P., Banschbach, J. L., & Yeagle, P. L. (1989c) *Biochemistry 28*, 5010–5019.

Thomas, E. L., Anderson, D. M., Henkee, C. S., & Hoffman, D. (1988) *Nature (London) 334*, 598–601.